RESEARCH ARTICLE

Elastic and Stretchable Double Network Hydrogel as Printable Ink for High-Resolution Fabrication of Ionic Skin

Kaiwen Chen†, Qiwei Ying†, Xingxing Hao†, Kai Sun, Huanan Wang*

Key State Laboratory of Fine Chemicals, School of Bioengineering, Dalian University of Technology, No. 2 Linggong Road, High-tech District, Dalian, 116024, P.R. China

†*These authors contributed equally to this work*

Abstract: A hydrogel that combines both printability and adaptability, high elasticity, and stretchability can provide ideal mechanical properties, and also render complex and accurate construction for ionic skin. However, it is extremely challenging. Here, we propose a colloidal-based double-network (DN) hydrogel as printable inks for high-precision fabrication of ionic skins. Particularly, polyacrylamide (PAAm), as the covalent network that can maintain the long-term material integrity, was combined with gelatin colloidal network to improve the injectability and printability of the resulting DN hydrogels. The DN design cooperatively provides the hydrogels with higher toughness values and deformability than what single colloidal or PAAm network can achieve. Further design of ionic skin based on capacitor microarray was demonstrated to serve as a sensitive and stable capacitor that can respond to external stimuli, thereby allowing to sense the body movements such as finger bending, laugh, and wrist pulse by translating mechanical changes into electric signals. Therefore, this study provides a novel strategy for the design and preparation of high-resolution ionic skins as the wearable sensor.

Keywords: Double-network hydrogel; Colloidal gel; 3D printing; Ionic skin; Capacitance microarray

*Correspondence to: Huanan Wang, Key State Laboratory of Fine Chemicals, School of Bioengineering, Dalian University of Technology, No.2 Linggong Road, High-tech District, Dalian, 116024, P.R.China; huananwang@dlut.edu.cn

Received: April 20, 2021 **Accepted:** May 25, 2021 **Published online:** June 25, 2021

(This article belongs to the *Special Section: Bioprinting of 3D Functional Tissue Constructs*)

Citation: Chen K, Ying Q, Hao X, *et al*., 2021, Elastic and Stretchable Double Network Hydrogel as Printable Ink for High-resolution Fabrication of Ionic Skin. *Int J Bioprint*, 7(3):377. http://doi.org/10.18063/ijb.v7i3.377

1. Introduction

Recently, various soft electronics have been developed to imitate skin's unique characteristics, such as mechanical adaptability and sensory capabilities[1]. These so-called "electronic skin" devices can convert external stimuli such as pressure[2], strain[3], and vibration[4] into reliable electronic signals, thus serving as ideal materials for the development of wearable devices and soft robotics. Although these electronic skins can sense various signals, they still show insufficient biocompatibility and mechanical adaptability which are caused by the potentially cytotoxic and rigid inorganic conductive materials. To this end, Whitesides *et al*. recently proposed the concept of "ionic skin" as biomimetic biosensor materials, in which mechanical signals can be converted into electric signals by using the soft, biocompatible, and ionically conductive hydrogels as the electronic conductors[5]. Unlike electronic skins composed of organic polymers and inorganic conductive materials, ionic skins typically consist of hydrophilic polymers dispersed in an aqueous salt solution that can transmit electrical signals through ions instead of electrons, resulting in physiological and mechanical properties comparable to natural skin tissues[6,7]. In general, the structure of the ionic skin is composed of a parallel plate capacitor and ionic hydrogel as the conductive layer. When the capacitor senses external stimuli (such as strain and pressure), the capacitance value will change. However, currently available ionic skins were

mostly based on chemically cross-linked hydrogels, such as polyacrylamide (PAAm). These hydrogels were inherently elastic, lack of stretchability and durability, and cannot adapt to the local movements of the human body[5]. Therefore, physically cross-linked hydrogels with self-healability and flexibility that can adapt to dynamic surfaces have been recently developed. However, these systems showed poor structural integrity, insufficient anti-fatigue properties, and plastic deformation under external force, which can compromise the materials stability and functionality of the ionic skins[8-11]. Therefore, it is still a challenge to develop hydrogel-based electronic sensors as ionic skins that feature the combined attributes of adaptability, high elasticity, and stretchability.

Gong *et al*. proposed double-network (DN) hydrogel, which typically combines a stable covalent network with a reversible non-covalent network, and has shown mechanical strength and toughness values orders of magnitude greater than what the can achieve separately[12-15]. Inspired by this concept, our group has developed DN hydrogels based on reversibly crosslinked colloidal network combined with a continuous phase of the permanently crosslinked network by covalent bonds. These hydrogels have shown significantly enhanced mechanical behavior, a high degree of stretchability and adaptability to local deformation or shear force[16]. Specifically, colloidal gels are based on a bottom-up assembly of micro- or nano-sized particles to form a porous but interconnected particulate network[17,18]. By introducing interparticle interactions such as electrostatic forces[19], magnetic forces[20], or hydrophobic interactions[21], and colloidal gels can develop shear-thinning and self-healing behavior, which are advantageous to applications in bioprinting, injectable scaffolds, or drug carriers.

Based on this design rationale, we hereby propose a DN colloidal hydrogel for the fabrication of ionic skins. Particularly, a binary composite hydrogel system composed of PAAm as the covalent network to maintain long-term material integrity in combination with a shear-thinning and self-healing gelatin colloidal network to improve the injectability and printability was developed, which allowed high-resolution fabrication of ionic skin with microscopic patterned microstructure by three-dimensional (3D) printing. The resulting DN ionic skin sensor can be rendered with high stretchability and elasticity, as well as enhanced sensitivity to forces and deformations, outperforming conventional bulk hydrogel-based ionic skins due to the specific microscale micro-architecture. The printed microarray in the current ionic skin devices can enable the sensing of the location where the external stress was applied with a resolution of millimeter-scale resolution (**Figure 1**). In general, we provide a novel approach for high-resolution fabrication of a new generation of ionic skin sensors with substantially higher stretchability and elasticity, which opens up a new avenue for the design and fabrication of degradable, implantable, and biocompatible smart electronics.

2. Materials and methods

2.1. Preparation of PAAm hydrogels

Acrylamide (AAm, 99%, Aladdin), N,N-methylene bis(acrylamide) (MBAA, 99%, Sigma-Aldrich), and 2-hydroxy-4'-(2-hydroxyethoxy)-2-methylpropiophenone (2959, >99%, Aladdin) were dissolved in 2 M NaCl solution at room temperature to obtain clear solution with different concentration of AAm (5 w/v%, 10 w/v% and 15 w/v%). The solution was further cross-linked by 365 nm ultraviolet (UV) lights (50 mW/cm^2, 60 s) to form PAAm hydrogels.

2.2. Preparation of colloidal hydrogels

Gelatin nanoparticles were prepared based on a previously reported two-step desolvation method[17]. Different mass fractions of gelatin nanoparticles (5%, 7.5%, 10%, and 15%) were dissolved in 2 M NaCl solution to obtain gelatin colloidal gels.

2.3. Preparation of DN hydrogels

For preparing the DN hydrogels, gelatin nanoparticles with a mass fraction of 10% were fully mixed with the solution which contained AAm as a monomer, MBAA as a crosslinking agent, and irgacure 2959 as a photo-initiator to obtain the colloidal gel. The AAm monomer in colloidal gel further was crosslinked by 365 nm UV lights (50 mW/cm^2, 60 s). The detailed parameters of hydrogels as listed in Table 1.

2.4. Scanning electron microscope (SEM)

The microstructure of hydrogels was observed by scanning electron microscopy (FEI, Quanta 450, USA). Specifically, the DN hydrogels were frozen and fractured at −80°C, and then freeze-dried to remove water. Then, the cross-sections of the hydrogel samples were coated with gold to increase the conductivity.

2.5. Rheology

The hydrogels were tested for rheological behavior using a discovery hybrid rheometer (DHR, TA instrument). The measurement was performed using a parallel plate fixture, and the gap distance was set to 1000 μm. The shear-thinning behavior of the colloidal gels was evaluated by a stepped flow test (shear rate was 0.1 – 100 1/s). The self-healing behaviors were quantitatively characterized by the change of storage modulus of the gels before/after destructive shearing (oscillatory strain sweep with an increased strain from 1 to 1000% and a frequency of 1 Hz for 200 s). The hydrogel samples were further

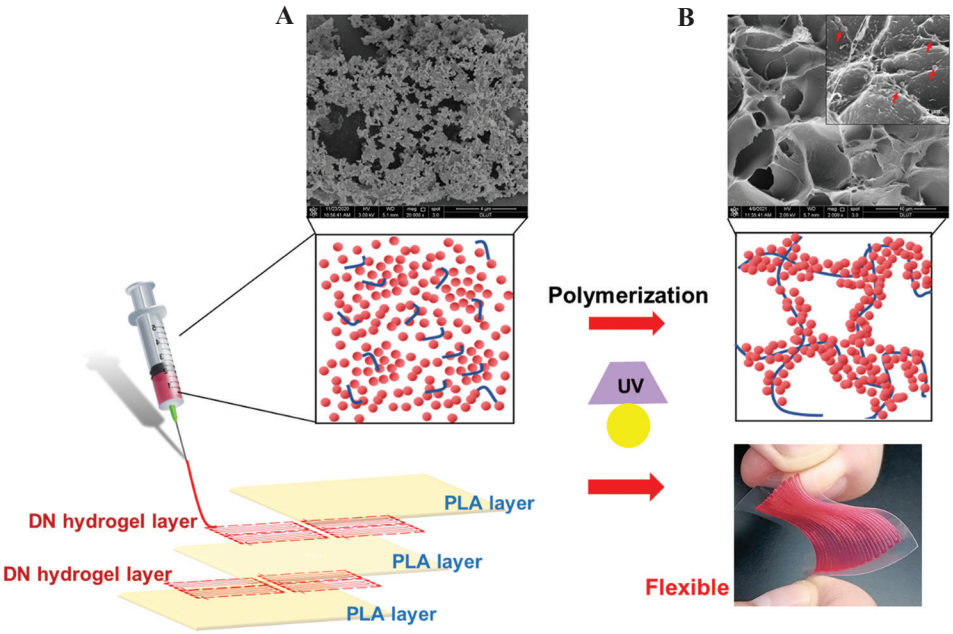

Figure 1. Design principle of gelatin/polyacrylamide (PAAm) double-network (DN) hydrogels for the preparation of ionic skin. The conductive layers were printed by gelatin nanoparticles in combination with AAm monomers, followed by photoinduced polymerization of PAAm, to obtain an elastic and flexible ionic skin. The dielectric layer was polylactic acid (PLA) film. The schematic diagram showing the mechanism of the formation of nanostructured gelatin colloidal network (A) and the DN hydrogels composed of gelatin nanoparticles and PAAm (B). Scanning electron microscope photographs showing the microstructures of pure gelatin colloidal gel and gelatin/PAAm DN hydrogels.

shaped by molding followed by secondary crosslinking by photo-induced polymerization of PAAm, in which the evolution of viscoelastic properties was determined by an oscillation time sweep (frequency of 1 Hz and strain of 0.5%). The inherent viscoelastic properties of the resulting hydrogels were characterized by an oscillation frequency sweep (0.1 to 100 rad/s at a constant strain of 0.5%).

2.6. Mechanical test

Compression and tensile test were performed using dumbbell-shaped and cylindrical-shaped specimens designed according to ISO standards and evaluated by a universal testing machine (E43, MTS instrument, USA) equipped with a 50 N sensor (25°C, 60% RH). The cyclic compression and tensile tests were carried out with a loading rate of 1 mm/min and samples were loaded to the initial deformation after being compressed to the strain of 0.75. The fracture energy (kJ/m^3) was calculated by the area below the tensile stress-strain curve used to characterize the work required to break a sample per unit volume. The elastic modulus was defined as the slope of the initial linear region of the stress-strain curve.

2.7. Printability and fidelity of DN hydrogels

To print the DN hydrogel, the hydrogel inks composed of gelatin nanoparticles and PAAm precursor solution were used to fabricate microstructures by a homemade extrusion-based bioprinter. Thereafter, the printed constructs were exposed to UV light to allow polymerization of PAAm. The injectability of the colloidal gels with different concentrations was evaluated by injecting force during the extrusion process by a universal testing machine (E43, MTS instrument, USA). Specifically, gelatin nanoparticles were weighed and mixed with 2 M NaCl solution (pH = 7.0) in 5 mL medical syringes (BD Plastipak™, orifice diameter of 400 μm) to obtain colloidal gels. After storing at 4°C for 2 h, the syringe was fixed vertically under the plate of the tensile bench, and a compressive force was applied to the plunger of the syringe at a constant velocity of 1 mm/min. The injection force was recorded as a function of the plunger travel time. In addition, the degree of material expansion after injection was evaluated by immediately recording photographs of the printed filaments from the nozzle of different diameters.

2.8. Fabrication of DN hydrogel-based ionic skin devices

To generate an ionic skin device with high resolution, we designed an electronic circuit with microarray printed by gelatin/PAAm DN hydrogel. Specifically, we used homemade 3D printing equipment, and 400 μm needle to further print DN hydrogel, and each sensor unit area is 7 mm × 7 mm, printing a total of 1 (1 × 1), 4 (2 × 2), and 49 (7 × 7) units of the ionic skin. To fabricate

a capacitor-based ionic skin, we first printed a hydrogel layer on a poly(lactic acid) (PLA) film layer, and hydrogel was further crosslinked to form a polymer network by 365 nm UV light. Then, we further printed a hydrogel layer on the top PLA layer and cured it with UV light, and the PLA film further covered as a dielectric layer and prevents evaporation of the hydrogel.

To further test the capacitance of capacitor-based ionic skin, we use an LCR meter (TH2830) at an AC voltage of 1 V and a sweeping frequency of 1 kHz. Capacitance changes were simultaneously detected with various stimuli on the prepared devices. The printed ionic skins were composed of five layers, of which the first, third, and fifth layers were PLA films (height: 50 μm), and the second and fourth layers were printed hydrogels.

3. Results and discussion

3.1. Mechanical properties of the DN hydrogels

The GNPs/PAAm DN hydrogels were prepared by directly mixing gelatin nanoparticles with flowable AAm monomer solution via multiple cycles of extrusion in a conventional medical syringe, followed by molding or printing into certain morphology that can be further photopolymerized to allow the solidification of the structures. Before triggering the polymerization of PAAm, we first evaluated the injectability and printability properties of pure nanostructured gelatin colloidal gels. By applying an increasing shear rate, the gelatin colloidal gels of different concentrations showed typical shear-thinning behavior as evidenced by a linear decrease in viscosity upon shearing (**Figure 2A**). Moreover, gelatin colloidal gels also showed a high degree of mechanical recovery after severe network destruction (or so-called self-healing behavior). As shown in **Figure 2B**, in the initial low strain region (0.5%), the colloidal gel showed the formation of a stable gel network as reflected by a higher value of G' than G". Subsequently, a higher shear strain (1 – 1000% for 1 min) led to network destruction and the transformation from a solid gel to a liquid-like material as reflected by G" higher than G'. On release of the destructive shear, gelatin colloidal gel immediately showed more than 70% of recovery of G' value as relevant to the initial G'. This can be attributed to the cohesive interactions between gelatin nanoparticles. Such shear-thinning and self-healing behavior rendered the colloidal gels printable and capable of blending with different components such as other types of micro-/nano-particles or flowable precursor solutions. To obtain a mechanically stable colloidal network, we prepared hydrogels containing gelatin nanoparticles with mass fraction ranging from 10 to 12 w/v% (corresponding to volume fraction above 0.5). Such highly packed colloidal systems can eliminate the effect resulting from the structural features of the particulate network on the mechanical properties of the resulting colloidal gels[22].

The gelatin/PAAm DN hydrogels not only maintained the shear-thinning and self-healing properties of the colloidal network but also exhibited enhanced gel elasticity after photopolymerization (G'~4 kPa) 3 times higher than before polymerization (**Figure 2C**). Further oscillatory frequency sweep tests revealed the frequency-independent behavior of the DN hydrogels as well as the colloidal gels; the DN gels had higher gel strength than the colloidal gels. In contrast, 10 w/v% PAAm hydrogels showed a more frequency-dependent behavior with the network moduli increasing gradually as a function of frequency (**Figure 2D**).

We further used conventional compression and tensile tests to characterize the mechanical properties of gelatin/PAAm DN hydrogels. On compression, the DN hydrogels initially showed a linear region with the stress increased linearly as strain increased (**Figure 3A**). After the linear region, the stress showed a sharp increase with increasing the compressive loading, with the compressive modulus E_c and strength σ_c of 31.1±4.6 and 270.1±15.7 kPa, respectively. Interestingly, we did not observe any yielding point even the compression strain was up to 95%, suggesting the considerable elasticity of the hydrogel matrix resulting from the DN design. In comparison, pure gelatin colloidal gels showed a similar elastic behavior at rather small deformation with the E_c = 32.9±4.5 and σ_c =15.7±1.8 kPa. However, gelatin colloidal gels can only resist 35% strain followed by an elastic fracture. Moreover, PAAm hydrogels showed a significantly weaker compressive modulus with E_c = 3.1±0.3 kPa as compared to both DN hydrogels and the colloidal gels.

Further tensile tests revealed almost purely elastic properties followed by an elastic fracture for the gelatin/PAAm DN hydrogels, evidenced by the highly linear stress-strain curve without showing any plastic deformation (**Figure 3B**). The tensile modulus E_t = 15.1±0.6 and tensile strength σ_t =27.8±1.3 kPa, respectively. Pure gelatin colloidal gel displayed a comparable tensile modulus E_t =14.1±3.1 but a considerably lower tensile strength σ_t =1.3±0.3 kPa as compared to DN hydrogels. In contrast, PAAm hydrogels showed the weakest mechanical properties with E_t = 2.3±0.4 and σt =2.5±0.2 kPa, respectively. Noticeably, the DN hydrogels also exhibited higher tensile fracture strain up to 1.74, slightly higher than PAAm (fracture strain of 1.21), but more than one order of magnitude higher than pure gelatin colloidal gels with yield strain of 0.11.

We further performed cyclic compression/tensile tests to explore the capacity of the DN hydrogels for anti-fatigue performance and energy dissipation on

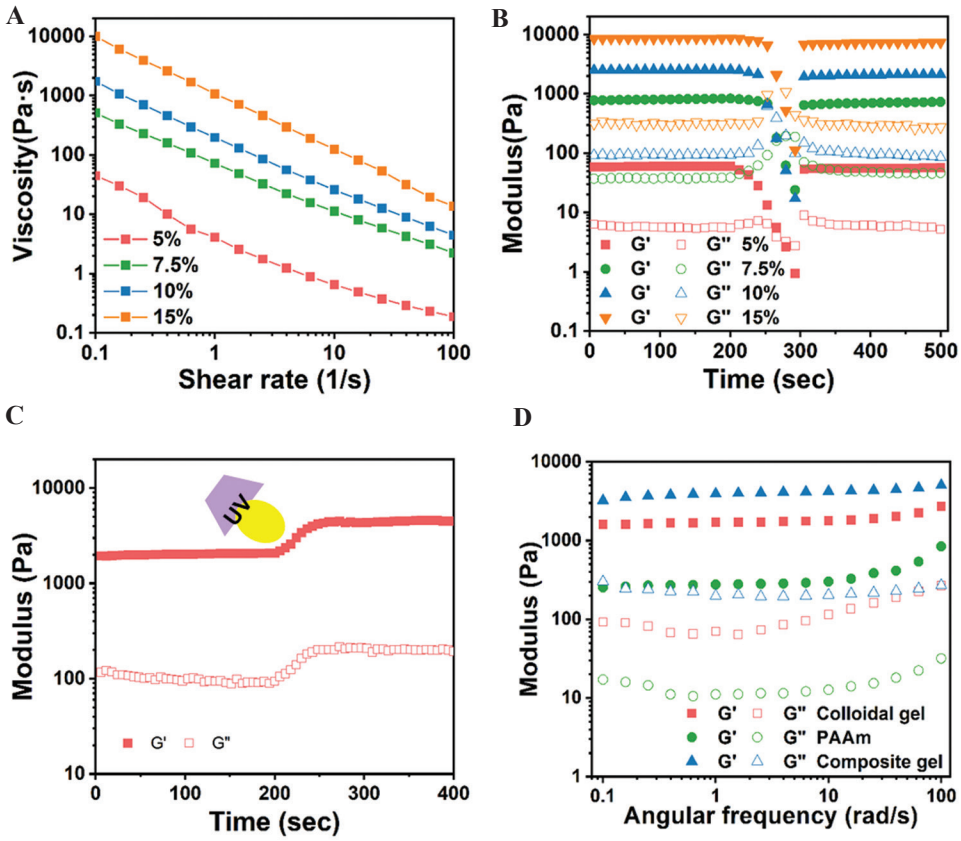

Figure 2. Viscoelastic properties of gelatin/polyacrylamide (PAAm) double-network (DN) hydrogels. (A) Shear-thinning behavior of the nanostructured gelatin colloidal gel of different concentrations (5, 7.5, 10, and 15 w/v%). (B) Evolution of modulus of the colloidal gel of different concentrations by applying the destructive shearing (oscillatory strain sweep with increasing strain from 1% to 1000% with a fixed frequency of 1 Hz) and the recovery (oscillatory time sweep at 0.5% strain and a frequency of 1 Hz for 200 s) on the release of destructive shearing. (C) Triggered photo-polymerization of gelatin/PAAm composite gels (time sweep at 0.5% strain and 1 Hz frequency), as reflected by the sharp increase of G' and G" values. (D) Frequency dependence of storage and loss modulus of pure gelatin colloidal gel (10 w/v% gelatin nanoparticles), PAAm (10w/v%), and gelatin/PAAm composite gel (10 w/v% gelatin nanoparticles, 10 w/v% PAAm).

loading. The gelatin/PAAm DN hydrogels can withstand the repetitive applications of the compressive stress of ~200 kPa and a compressive strain up to 0.75, and can rapidly recover to the original shape upon unloading during the cyclic compression test (**Figure 3C**). For the cyclic tensile tests, the DN hydrogels also showed a wide-range linear elasticity and capability to resist repetitive tensile stress of ~15 kPa and a tensile strain of 1 (**Figure 3D**). Similarly, we observed almost complete recovery to the original state on unloading and overlapped hysteresis loops even after 50 cycles of loading/unloading. These findings suggest that the DN hydrogels are highly elastic and anti-fatigue, which are of significant importance for the development of wearable devices that adapt to body movements[23,24].

We compared the current colloidal-based DN hydrogels with previously reported highly strong or tough hydrogels. Typical DN hydrogels achieve high robustness or toughness values through the combination of a permanent covalent network with a reversibly crosslinked non-covalent network to allow energy dissipation[14], thereby realizing gel mechanics outperforming what they can achieve individually. However, the preparation of conventional DN hydrogels was normally time-consuming and complicated, which restricted the precision manufacturing and wide-spreading applications[13]. Alternative strategy of introducing nanoparticles as the reinforcement components to the continuous polymer network was widely-used to prepare strong hydrogels as compared to the DN design, which normally confronted with the issue of network homogeneity of the disperse and continuous phases, and subsequent compromised mechanical properties[25]. In comparison, our DN design based on colloidal and polymeric networks combined the superior properties of both components, including ease of preparation, injectability, or moldability rendered by the reversibly crosslinked colloidal network, and high network mechanics and structural integrity resulting from the covalent PAAm network. Such combination allows us to fabricate these hydrogels into micro-meter scale

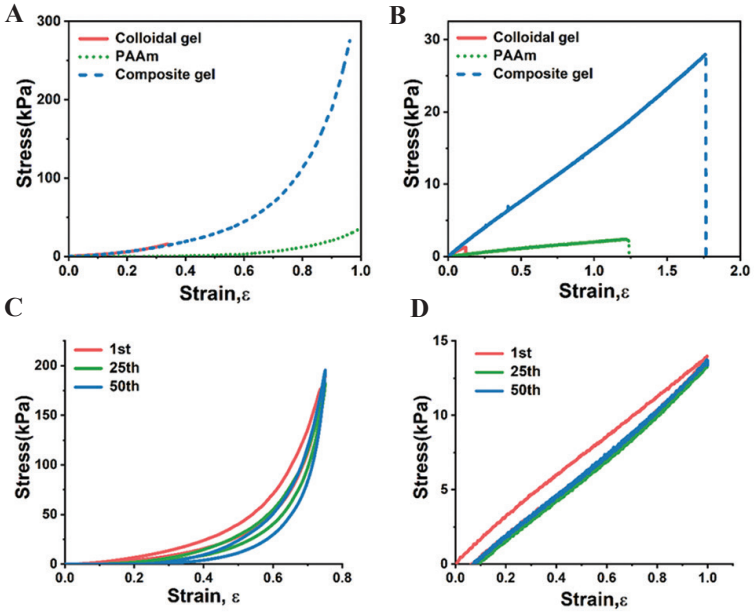

Figure 3. The mechanical properties of double-network (DN) hydrogels tested using conventional compressive and tensile tests. The stress-strain curves of (A) compressive and (C) tensile measurements at a strain rate of 0.021 1/s for the gelatin colloidal gel, polyacrylamide (PAAm), and gelatin/PAAm DN hydrogels. The hysteresis curves of DN hydrogels on (B) cyclic compressive and (D**)** tensile loading and unloading.

resolution through 3D printing meanwhile achieving outstanding gel mechanics through secondary crosslinking based on photo-polymerization of the polymer phase.

3.2. Printability of the DN hydrogels

We further evaluated the printability of the DN hydrogels as inks for 3D printing. Typically, we first assessed the injectability of the hydrogel inks by monitoring the compressive force for the extrusion of the inks using conventional medical syringes (**Figure 4A**). It was shown that gelatin hydrogel in with different colloid concentrations of 5, 7.5, and 10 w/v% can be easily extruded with a rather low compressive force (<20 N). In comparison, a higher colloid concentration (15w/v%) in the inks showed difficulty to extrude the inks out of the nozzle, with continuously increased compressive force up to 35 N. Moreover, images showing the shapes of the inks extruded out of the nozzles of the syringes showing different flow patterns during the injection (**Figure 4B**). Only inks containing 7.5-10 w/v% gelatin colloids still retained a noodle-like shape after injection, indicating the formation of stable flow during shear-thinning process. In contrast, both inks containing lower or higher concentrations of gelatin colloids formed drop-like shapes on injection. The former condition can be related to too dilute colloid concentration to allow fluent injection, while the latter can be related to too densely pack colloidal network that jammed in the syringe and led to poor injectability. We further observed the inks to expand when they were extruded out of the nozzle due to the release of shear stress, for which we can compare the change of the diameters of the injected strands as relative to the original nozzle diameter to evaluate the capacity of the inks to facilitate precise microfabrication. As a result, inks containing 10 w/v% colloids showed an expansion rate of ~120% when using a nozzle with a diameter of 200 μm, which was half to that of the 7.5 w/v% colloids (~240%) (**Figure 4C** and D). This can be explained by the tendency of the dilute colloidal components to stress-relax after being released from the confinement from the nozzle.

To demonstrate high-resolution printing using gelatin/PAAm DN hydrogel ink, we fabricated a connected circuit device using the hydrogel to form more than 49 patterned sub-units in a 50 mm × 50 mm area. A nozzle size of 400 μm was used, and resolution of the device preparation can reach up to 800 μm (**Figure 5A and B**). Such high-resolution construction of microarray architecture can allow high-degree sensitivity of the spatial location with the circuit area where pressure or deformation was applied. Moreover, we also printed an ear-shape construct using our DN hydrogel ink and observed that the sharp and rounded corners can be precisely fabricated, confirming the fidelity of the gelatin/PAAm DN hydrogel-based inks (**Figure 5C and D**).

3.3. 3D printed capacitance devices as wearable devices using the DN hydrogel

Typically, the hydrogel-based capacitor senses the pressure by the change in the relative area of conductive

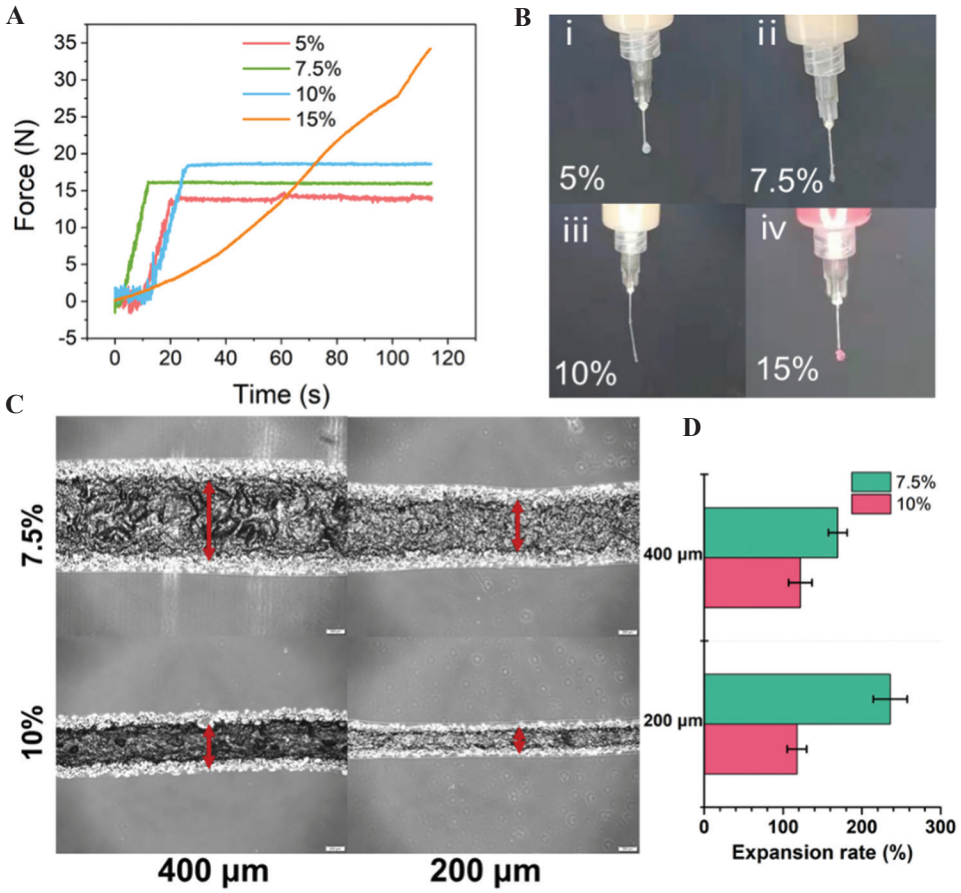

Figure 4. (A) Injectability of gelation colloidal gels (5, 7.5, 10, and 15 w/v % solid content) by measuring the compression force as a function of time during injection of the hydrogels using medical syringes. (B) Photographs showing the injectability of 5, 7.5, 10, and 15 w/v% gelatin colloidal gels during the injection test. (C) The light microscopic images showing the strands formed by gelatin colloidal gels (7.5, 10 w/v%) injected by syringes with different nozzle diameter (200 and 400μm). (D) Quantitative analysis of the expansion rate calculated by the ratio of the hydrogel strands after extrusion as relative to the original nozzle size.

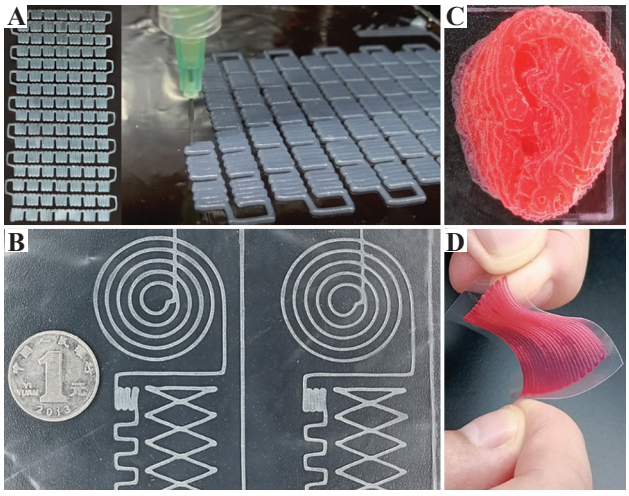

Figure 5. (A and B) Photographs showing the patterned electronic circuit printed by gelatin/polyacrylamide double-network (DN) hydrogel. (C) The ear-shaped construct was printed by DN hydrogel. (D) Image showing the high flexibility and stability of the printed patterned electronic circuit on a PLA film.

hydrogels. The relationship between deformation and capacitance in a parallel-plate capacitor can be explained by the equation $C = \varepsilon S/4\pi kd$, where C is the capacitance, ε is the dielectric constant, k is the electrostatic constant, S is the effective area of the conducting layer, and d is the thickness of the dielectric layer. Based on this theory, the expansion of the cross-section area of a hydrogel ionic skin can lead to increasing capacitance. Therefore, to prepare a capacitor as ionic skin, we printed a layer of electronic circuit array using DN hydrogels on the surface of a dielectric PLA film followed by printing another layer of electronic circuit array arranged orthogonally to the first printed layer (**Figure 6A**). Another two layers of PLA films were used as insulator layers to cover the conductive hydrogels and prevent the moisture from evaporation. To demonstrate the sensitivity of the ionic skins, we pressed the microarray using finger-touch or monitored complicated muscle movements. We used acrylic elastomer tape to adhesion the ionic skin to the finger. The two-layer ionic hydrogel's contact

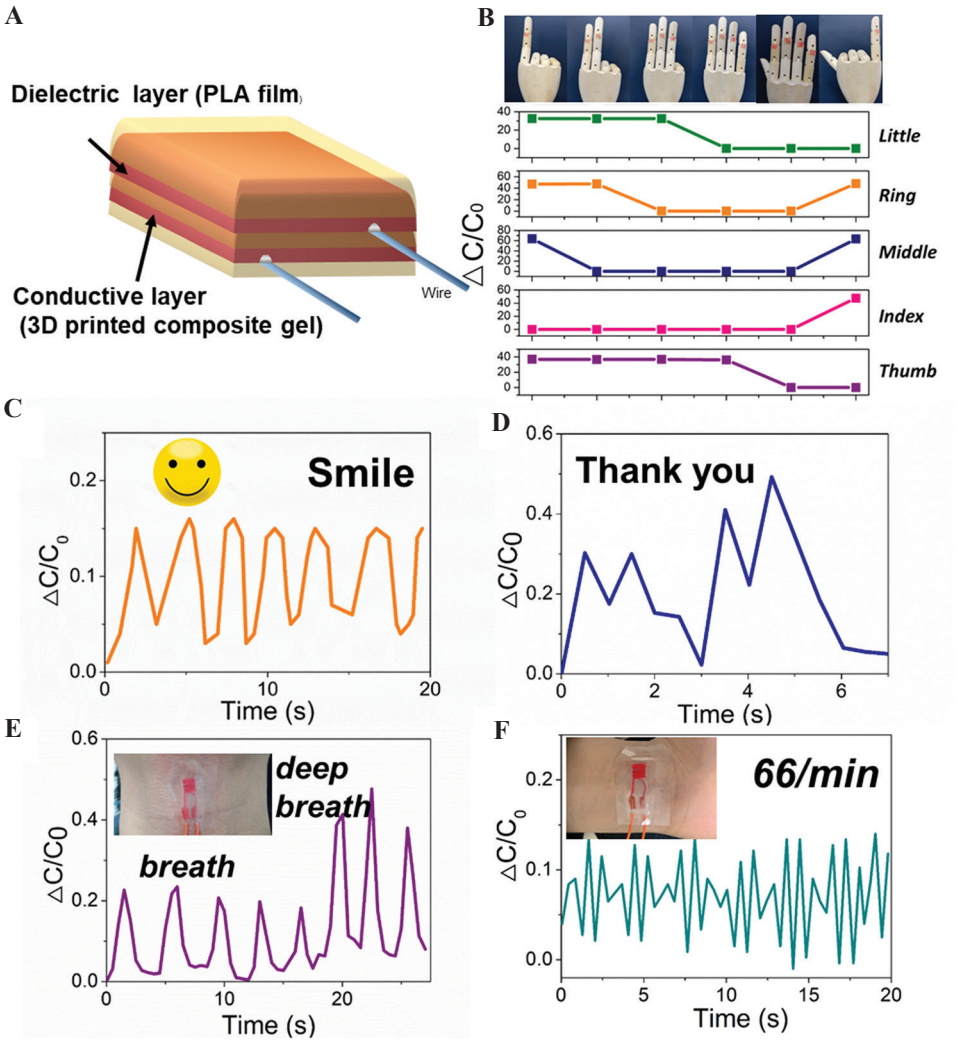

Figure 6. (A**)** Schematic design of the ionic skin developed in the current study. (B) The printed hydrogel sensors attached to a puppet hand and the real-time capacitance signals when different gestures were posed. Inserted images showing the corresponding gestures of the puppet hand. Real-time capacitance signals when the tester who wore the device (C) laughed, **(**D) said "thank you," and (E) took deep breaths. (F) Real-time capacitance signals of pulse when the sensor attaches to the tester's wrist.

area increased when the finger bending, leading to an increase in capacitance (**Figure 6B**). When the ionic skin was attached to the throat, it exhibited repeatable and characteristic signal peaks as the tester laughed or spoke (**Figure 6C and D**). The ionic skins also can distinguish between breathing and deep breathing by the degree of deformation on being worn on the chest of the tester (**Figure 6E**). Moreover, we also proved the application of this ionic skin as a sensor for wrist pulse. The capacitance changes showed periodic fluctuations according to the rhythm of pulse beating (**Figure 6F**). All these applications confirmed that these DN hydrogel-based ionic skins were promising candidates as highly sensitive pressure and strain sensors for wearable devices. To further evaluate the applications of the printed ionic skin in the flexible smart devices, a flexible touch screen panel (7×7 sensors, 5×5 mm^2 square per sensor unit) was fabricated to map the location of applied pressure with high resolution (**Figure 7A**). When one finger or two fingers touch the screen, the corresponding pressure peak mapping can be generated by measuring all the capacitance of the subunits (**Figure 7B**). Moreover, by placing cross- or box-shaped plastic devices on the touch screen panel's surface, we can locate the position and shapes of the devices placed.

For the development of a human-computer interaction monitor, a set of miniaturized functional chips were utilized, including printed ionic skin, data collector, control system, data transition, main control board, and output device (**Figure 8A**). The capacitance value of ionic skin will increase under external pressure, thus we can transfer the capacity signal to other signals,

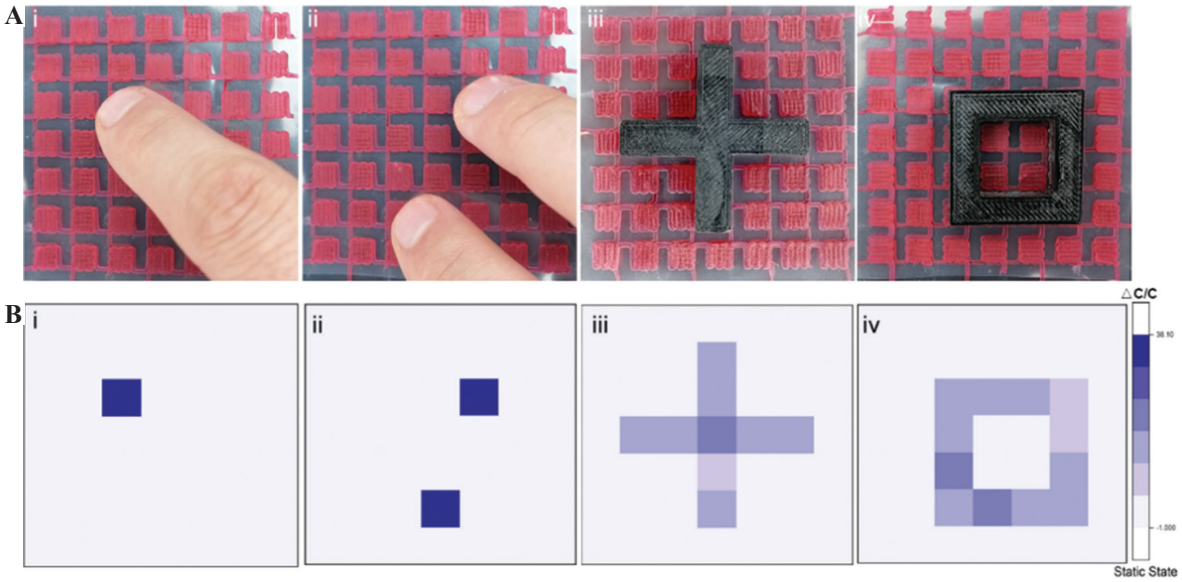

Figure 7. Sensitivity of the printed electronic circuit pattern. (A) Images showing the position of finger-touch (i, ii) and the placing of complex structures (iii, iv) on top of the printed ionic skin array, and (B) the corresponding capacitance signals based on the sensing of the different pressure mapping.

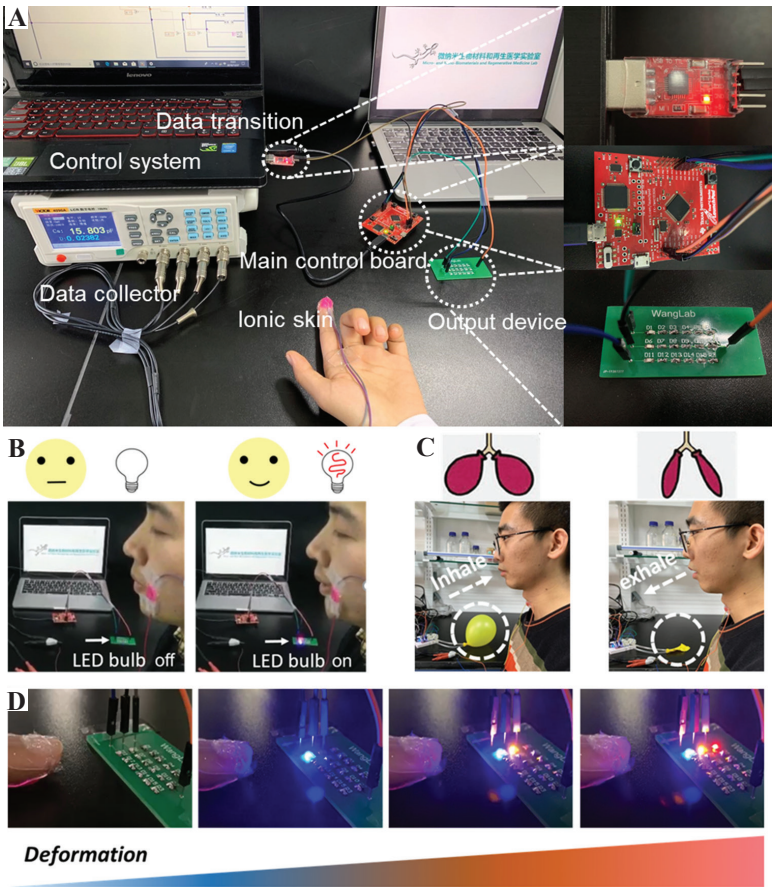

Figure 8. Human-computer interaction based on the ionic skin. (A) Human-computer interaction platform, including the printed ionic skin, data collector, control system, data transition, main control board, and output device. (B) The ionic skin device was attached to the tester's face, and controlled the LED bulb to turn on when the tester smiled **(**C) The ionic skin device was attached to the tester's throat, and controlled the inflation and deflation of the balloon when the tester was breathing. (D) The ionic skin device was attached to the finger to control different LED bulbs to turn on and off by different levels of pressure.

Table 1. Contents of DN hydrogel

Samples	AAM	GNPs	MBAA	2959	NaCl solution (2M)
5% colloidal gel	0 mg	150 mg	0 mg	0 mg	3 ml
7.5% colloidal gel	0 mg	225 mg	0 mg	0 mg	3 ml
10% colloidal gel	0 mg	300 mg	0 mg	0 mg	3 ml
15% colloidal gel	0 mg	450 mg	0 mg	0 mg	3 ml
5% PAAm hydrogel	150 mg	0 mg	1.5 mg	15 mg	3 ml
10% PAAm hydrogel	300 mg	0 mg	3 mg	15 mg	3 ml
15% PAAm hydrogel	450 mg	0 mg	4.5 mg	15 mg	3 ml
10% PAAm composite hydrogel	300 mg	300 mg	3 mg	15 mg	3 ml
15% PAAm composite hydrogel	450 mg	300 mg	4.5 mg	15 mg	3 ml

PAAm: Polyacrylamide; DN: Double-network

such as light and mechanical signals. As an example, the ionic skin was mounted on the tester's face, when the tester smiled, the capacity of ionic skin increased, and correspondingly controlled the LED bulb on and off (**Figure 8B**). Furthermore, by adhering the ionic skin to the tester's throat, we can control the inflation and deflation of a balloon by the inhalation and exhalation of the tester. For patients with breathing difficulties and breathing disorders, we suggested that this design can potentially test the inspiratory and expiratory volumes during breathing of the patients (**Figure 8C**). We further put the ionic skin on the fingertips of the tester and used the finger to compress the substrate with different levels of forces, through which the ionic skin can generate different degrees of deformation and capacitance values; this can be further converted to a readout signal. The increase of capacity signal can cause the LEDs to light up, and the number of lit LEDs corresponded to the degree of the applied pressure (**Figure 8D**).

4. Conclusion

In summary, we hereby presented the development of a novel class of DN hydrogels as printable skins for the fabrication of ions skin devices. The DN hydrogels were based on reversible gelatin colloidal network in combination with covalent PAAm network, which showed rapid, customized, and high-resolution fabrication of microscale constructs as ionic skins. The DN hydrogel displayed significantly enhanced elasticity and deformability which allow high adaptability of the resulting ionic skin devices to the body's movements. We further used the DN hydrogel to print microarray-based capacitors as ionic skins with high elasticity, stretchability, and sensitivity. The ionic skins exhibited high sensitivity to gentle finger-touch, body motion, and even wrist pulse-beating. We believe that this ionic skin can be potentially applied in the fields of human/machine interactions and wearable devices, and can promote the development of next-generation intelligent skin-mimicking sensors.

Acknowledgments

This work was supported by the National Key Research and Development Program of China (No.2018YFA0703000), National Natural Science Foundation of China (No. 31870957), and the Fundamental Research Funds for the Central Universities of China (No. DUT15RC(3)113).

Conflict of interest

The authors declare no conflict of interest.

Author contributions

K.C. and H.W. designed the study. K.C., Q.Y., and X.H. performed the experiments and analyzed the results. K.C., Q.Y., and H.W. wrote the manuscript. All authors commented on the manuscript.

References

1. Wang X, Dong L, Zhang H, *et al*., 2015, Recent Progress in Electronic Skin. *Adv Sci* (*Weinh*), 2:1500169. http://dx.doi.org/10.1002/advs.2015001691
2. Chortos A, Liu J, Bao Z, 2016, Pursuing Prosthetic Electronic Skin. *Nat Mater*, 15:937–50. http://dx.doi.org/10.1038/nmat46712
3. Jeon J, Lee HB, Bao Z, 2013, Flexible Wireless Temperature Sensors Based on Ni Microparticle-filled Binary Polymer Composites. *Adv Mater*, 25:850–5. http://dx.doi.org/10.1002/adma.2012040823
4. Chortos A, Bao Z, 2014, Skin-inspired Electronic Devices. *Mater Today*, 17:321–31. http://dx.doi.org/10.1016/j.mattod.2014.05.0064
5. Sun JY, Keplinger C, Whitesides GM, *et al*., 2014, Ionic Skin. *Adv Mater*, 26:7608–14. http://dx.doi.org/10.1002/adma.2014034415
6. Wen J, Tang J, Ning H, *et al*., 2021, Multifunctional Ionic Skin with Sensing, UV-Filtering, Water-Retaining, and Anti-

Freezing Capabilities. *Adv Funct Mater*, 31:2011176. http://dx.doi.org/10.1002/adfm.2020111766

7. Zhou Y, Wan C, Yang Y, *et al*., 2019, Highly Stretchable, Elastic, and Ionic Conductive Hydrogel for Artificial Soft Electronics. *Adv Funct Mater*, 29:1806220. http://dx.doi.org/10.1002/adfm.2018062207
8. Chen K, Lin Q, Wang L, *et al*., 2021, An All-in-One Tannic Acid-Containing Hydrogel Adhesive with High Toughness, Notch Insensitivity, Self-Healability, Tailorable Topography, and Strong, Instant, and On-Demand Underwater Adhesion. *ACS Appl Mater Interfaces*, 13:9748–61. http://dx.doi.org/10.1021/acsami.1c006378
9. Lei Z, Wu P, 2019, A Highly Transparent and Ultra-stretchable Conductor with Stable Conductivity during Large Deformation. *Nat Commun*, 10:3429. http://dx.doi.org/10.1038/s41467-019-11364-w9
10. Lei Z, Wang Q, Sun S, *et al*., 2017, A Bioinspired Mineral Hydrogel as a Self-Healable, Mechanically Adaptable Ionic Skin for Highly Sensitive Pressure Sensing. *Adv Mater*, 29:22. http://dx.doi.org/10.1002/adma.20170032110
11. Lei Z, Huang J, Wu P, 2019, Traditional Dough in the Era of Internet of Things: Edible, Renewable, and Reconfigurable Skin-Like Iontronics. *Adv Funct Mater*, 30:1908028. http://dx.doi.org/10.1002/adfm.20190801811
12. Sun JY, Zhao X, Illeperuma WR, *et al*., 2012, Highly Stretchable and tough Hydrogels. *Nature*, 489:133–6. http://dx.doi.org/10.1038/nature1140912
13. Gong JP, Katsuyama Y, Kurokawa T, *et al*., 2003, Double-Network Hydrogels with Extremely High Mechanical Strength. *Adv Mater*, 15:1155–8. http://dx.doi.org/10.1002/adma.20030490713
14. Gong JP, 2010, Why are Double Network Hydrogels so Tough? *Soft Matter*, 6:2583–90. http://dx.doi.org/10.1039/b924290b1.
15. Chen K, Feng Y, Zhang Y, *et al*., 2019, Entanglement-Driven Adhesion, Self-Healing, and High Stretchability of Double-Network PEG-Based Hydrogels. *ACS Appl Mater Interfaces*, 11:36458–68. http://dx.doi.org/10.1021/acsami.9b1434815
16. Mu Z, Chen K, Yuan S, *et al*., 2020, Gelatin Nanoparticle-Injectable Platelet-Rich Fibrin Double Network Hydrogels with Local Adaptability and Bioactivity for Enhanced Osteogenesis. *Adv Healthc Mater*, 9:e1901469. http://dx.doi.org/10.1002/adhm.20190146916
17. Wang H, Hansen MB, Lowik DW, *et al*., 2011, Oppositely Charged Gelatin Nanospheres as Building Blocks for Injectable and Biodegradable Gels. *Adv Mater*, 23:H119–H124. http://dx.doi.org/10.1002/adma.20100390817
18. Wang H, Boerman OC, Sariibrahimoglu K, *et al*., 2012, Comparison of Micro- vs. Nanostructured Colloidal Gelatin Gels for Sustained Delivery of Osteogenic Proteins: Bone Morphogenetic Protein-2 and Alkaline Phosphatase. *Biomaterials*, 33:8695–703. http://dx.doi.org/10.1016/j.biomaterials.2012.08.02418.
19. Du M, Liu P, Wong JE, *et al*., 2020, Colloidal Forces, Microstructure and Thixotropy of Sodium Montmorillonite (SWy-2) Gels: Roles of Electrostatic and van der Waals Forces. *Appl Clay Sci*, 195:105710. http://dx.doi.org/10.1016/j.clay.2020.10571019
20. Komarov KA, Yurchenko SO, 2020, Colloids in rotating electric and magnetic fields: Designing tunable interactions with spatial field hodographs. *Soft Matter*, 16:8155–68. http://dx.doi.org/10.1039/d0sm01046d20
21. Ruter A, Kuczera S, Gentile L, *et al*., 2020, Arrested Dynamics in a Model Peptide Hydrogel System. *Soft Matter*, 16:2642–51. http://dx.doi.org/10.1039/c9sm02244a21
22. Diba M, Wang H, Kodger TE, *et al*., 2017, Highly Elastic and Self-Healing Composite Colloidal Gels. *Adv Mater*, 29:11. http://dx.doi.org/10.1002/adma.2016046721
23. Huang H, Han L, Li J, *et al*., 2020, Super-stretchable, Elastic and Recoverable Ionic Conductive Hydrogel for Wireless Wearable, Stretchable Sensor. *J Mater Chem A*, 8:10291–300. http://dx.doi.org/10.1039/d0ta02902e22
24. Pan Z, Yang J, Li L, *et al*., 2020, All-in-one Stretchable Coaxial-fiber Strain Sensor Integrated with High-performing Supercapacitor. *Energy Storage Mater*, 25:124–30. http://dx.doi.org/10.1016/j.ensm.2019.10.02323
25. Haraguchi K, 2007, Nanocomposite Hydrogels. *Curr Opin Solid State Mater Sci*, 11:47–54. http://dx.doi.org/10.1016/j.cossms.2008.05.0013